

## Article

# Spectrochemical determination of unique bacterial responses following long-term low-level exposure to antimicrobials

Jin, Naifu, Semple, Kirk T., Jiang, Longfei, Luo, Chunling, Martin, Francis L and Zhang, Dayi

Available at <http://clock.uclan.ac.uk/22011/>

*Jin, Naifu, Semple, Kirk T., Jiang, Longfei, Luo, Chunling, Martin, Francis L ORCID: 0000-0001-8562-4944 and Zhang, Dayi (2018) Spectrochemical determination of unique bacterial responses following long-term low-level exposure to antimicrobials. Analytical Methods, 10 . pp. 1602-1611. ISSN 1759-9660*

It is advisable to refer to the publisher's version if you intend to cite from the work.

<http://dx.doi.org/10.1039/c8ay00011e>

For more information about UCLan's research in this area go to <http://www.uclan.ac.uk/researchgroups/> and search for <name of research Group>.

For information about Research generally at UCLan please go to <http://www.uclan.ac.uk/research/>

All outputs in CLoK are protected by Intellectual Property Rights law, including Copyright law. Copyright, IPR and Moral Rights for the works on this site are retained by the individual authors and/or other copyright owners. Terms and conditions for use of this material are defined in the <http://clock.uclan.ac.uk/policies/>

1 **Spectrochemical determination of unique bacterial responses following long-term low-**  
2 **level exposure to antimicrobials**

3 Naifu Jin<sup>a,b</sup>, Kirk T Semple<sup>a</sup>, Longfei Jiang<sup>c</sup>, Chunling Luo<sup>c</sup>, Francis L Martin<sup>d,\*</sup>, Dayi  
4 Zhang<sup>a,b,\*</sup>

5 *<sup>a</sup>Lancaster Environment Centre, Lancaster University, Lancaster LA1 4YQ, UK*

6 *<sup>b</sup>School of Environment, Tsinghua University, Beijing 100084, China*

7 *<sup>c</sup>Guangzhou Institute of Geochemistry, Chinese Academy of Sciences, Guangzhou 510640,*  
8 *China*

9 *<sup>d</sup>School of Pharmacy and Biomedical Sciences, University of Central Lancashire, Preston*  
10 *PR1 2HE, UK*

11

12 **\*Corresponding authors:**

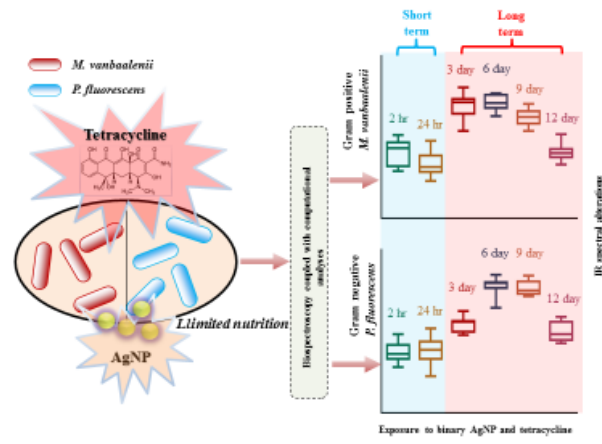
13 Francis L Martin, School of Pharmacy and Biomedical Sciences, University of Central  
14 Lancashire, Preston PR1 2HE, UK; Email: [flmartin@uclan.ac.uk](mailto:flmartin@uclan.ac.uk)

15 Dayi Zhang, School of Environment, Tsinghua University, Beijing 100084, China; Email:  
16 [zhangdayi@tsinghua.org.cn](mailto:zhangdayi@tsinghua.org.cn)

17

18 ToC graphic

19



20

21

## 22 **Abstract**

23 Agents arising from engineering or pharmaceutical industries may induce significant  
24 environmental impacts. Particularly, antimicrobials not only act as efficient eliminators of  
25 certain microbes but also facilitate the propagation of organisms with antimicrobial resistance,  
26 raising critical health issues, *e.g.*, the bloom of multidrug-resistant bacteria. Although many  
27 investigations have examined microbial responses to antimicrobials and characterized  
28 relevant mechanisms, they have focused mainly on high-level and short-term exposures,  
29 instead of simulating real-world scenarios in which the antimicrobial exposure is at a low-  
30 level for long periods. Herein, we developed a spectrochemical tool, attenuated total  
31 reflection Fourier-transform infrared (ATR-FTIR) spectroscopy, as a high-throughput and  
32 nondestructive approach to interrogate the long-term effects of low-level antimicrobial  
33 exposure in bacterial cells. Post-exposure to nanoparticulate silver (AgNP), tetracycline or  
34 their mixtures for 12 days, Gram-positive (*Mycobacterium vanbaalenii* PYR-1) and Gram-  
35 negative (*Pseudomonas fluorescens*) bacteria exhibited distinct IR spectral alterations.  
36 Multivariate analysis coupled with multivariate regression tree (MRT) indicates nutrient  
37 depletion and exposure time as the primary factors in bacterial behaviour, followed by  
38 exposure category and bacterial type. Nutrient depletion and starvation during long-term  
39 exposure drives bacterial cells into a dormant state or to exhibit additional cellular  
40 components (*e.g.*, fatty acids) in response to antimicrobials, consequently causing a broader  
41 range of spectral alterations compared to short-term exposure. This work is the first report  
42 highlighting the more important roles of exposure duration and nutrient depletion, instead of  
43 treatment regimen of antimicrobial, on microbial responses to low-level and prolonged  
44 environmental exposures.

45

## 46 1. Introduction

47 Environmental exposure to antimicrobials is a critical issue for both human and microbial  
48 communities. Antibiotics are currently ranked as the third most commonly prescribed drugs<sup>1</sup>.  
49 In human and veterinary medicine there is abuse of antibiotics, especially for keeping animals  
50 healthy at a sub-therapeutic level<sup>2-9</sup>. The primary sink for such antibiotic usage is the  
51 environment, *e.g.*, waters and soils, *via* various pathways post-excretion<sup>2, 3 4, 6</sup>. Another group  
52 of frequently-used antimicrobial agents is silver-associated entities. Notably, unlike silver ion  
53 or salts whose antimicrobial effects are well-studied, the mechanisms of nanoparticulate  
54 silver (AgNP) activity remain unclear. However, AgNP is widely exploited for its  
55 antibacterial activity, in clothing, food containers, wound dressings, ointments, implant  
56 coatings, and ultrafiltration membranes for water purification<sup>10-14</sup>. Developing a reliable  
57 approach to interrogate microbial responses to antimicrobials is therefore a matter of urgency,  
58 contributing to better understanding of the mechanisms and impacts of antimicrobial agents  
59 on environmental microbes<sup>15</sup>.

60 A major issue is the translation from laboratory culture to the real-world scenario of  
61 bacteria living in their natural habitats. In contrast to most laboratory culture conditions, *e.g.*,  
62 nutrient rich broth, free-living bacteria commonly face nutrient depletion or even more  
63 prohibitive circumstances<sup>16</sup>. For instance, cells inhabiting biofilm may be exposed to  
64 different concentrations of nutrients, metabolites or environmental stimuli (*e.g.*, temperature,  
65 pH, oxygen, etc.)<sup>17-21</sup> across the biofilm matrix and local microenvironment, leading to  
66 heterogeneous growth rates and behaviours amongst the cell populations<sup>22, 23</sup>. Amongst these,  
67 a small proportion might differentiate into a highly protected phenotypic state and coexist  
68 with neighbouring populations that are antibiotic sensitive, resulting from inherent strain  
69 differences and adaptation to relatively low concentrations of exposure<sup>16, 22, 23</sup>. Moreover,  
70 although regulatory agencies and pharmaceutical administration generally employs high  
71 doses of antimicrobials in *in-vivo* and *in-vitro* trials to ensure the safety of test chemicals,  
72 residual exposure is typically associated with extremely low-levels in the physical  
73 environment; this raises question as to whether high-concentrations of exposure represent the  
74 real-world outcomes<sup>24-29</sup>. Thus, research on prolonged low-level exposures of antimicrobials  
75 is required in order to shed deeper insights into microbial responses to antimicrobials in the  
76 real-world environment<sup>15</sup>.

77 Despite recently developed molecular techniques towards targeting microbial  
78 phenotypes, such approaches to identify minor or pre-stage phenotypic alterations induced by  
79 low-level exposure remain limited<sup>30-33</sup>. Meanwhile, other confounding factors (*e.g.*, microbial  
80 species, growth phase, exposure time, etc.) may also influence test results<sup>16, 31, 34</sup>. In 1991,  
81 Fourier-transform infrared (FTIR) spectroscopy was innovatively introduced as a sensitive  
82 and rapid screening tool for the characterization, classification and identification of  
83 microorganisms<sup>16</sup>. Since then, the emerging application of spectrochemical techniques with  
84 computational analysis as an inter-discipline approach shows promising feasibility in  
85 microbiology and cytology<sup>30-36</sup>. In the last decade, FTIR spectroscopy plus chemometrics has  
86 been exploited broadly for identifying microbial identities, physiologies, activities and related  
87 functions<sup>16, 30, 31, 33, 34, 37, 38</sup>. This technical combination provides a major advantage in terms  
88 of being high-throughput, label-free and cost-effective in application<sup>30</sup>, allowing one to  
89 interrogate biological samples *via* a nondestructive and nonintrusive manner, which has great  
90 potential in monitoring real-world scenarios<sup>30-32, 34</sup>.

91 The current study applied attenuated total reflection FTIR (ATR-FTIR) microscopy  
92 coupled with multivariate analysis to investigate bacterial responses to prolonged low-level  
93 exposures of AgNP and tetracycline under nutrient depletion conditions. Compared to short-  
94 term exposure, we found that length of exposure plays a more important role than treatment  
95 with antimicrobial reagents or bacterial type, further uncovering key influential factors of  
96 bacterial responses to antimicrobials during cell growth associated with nutrient depletion.

## 97 **2. Methodology**

### 98 *2.1 Cell strains and sample preparation*

99 The two bacterial strains used in this study were *Mycobacterium vanbaalenii* PYR-1 (Gram-  
100 positive; originally isolated by Carl E Cerniglia and stored in the culture collection  
101 <https://www.dsmz.de/catalogues/details/culture/DSM-7251.html>) and *Pseudomonas*  
102 *fluorescens* (Gram-negative; originally isolated in the laboratory of Kirk T Semple at  
103 Lancaster University and gifted for purposes of this study). They were both grown in minimal  
104 medium with 20 mM sodium succinate, undertaken in a dark rotary shaker at 150 rpm and the  
105 culture temperature was 30±2°C. After centrifugation and washing with sterile water, cell  
106 pellets were diluted in fresh minimal medium with 20 mM sodium succinate and cultivated  
107 for about 2 h until they reached the early log-phase (CFU=1×10<sup>7</sup> cells/mL). The four  
108 treatments included non-exposure negative control (CK), 4 µg/L of AgNP, 1 µg/L of

109 tetracycline, and a mixture with 4  $\mu\text{g/L}$  of AgNP and 1  $\mu\text{g/L}$  of tetracycline (Binary). The  
110 concentrations of AgNP and tetracycline were selected according to their previous reported  
111 level in natural environment to mimic the low-level exposure in real-world scenario<sup>38</sup>. They  
112 are about 2-4 orders of magnitude lower than the minimum inhibitory concentration (MIC) of  
113 AgNP (1 to 10 mg/L)<sup>39, 40</sup> and tetracycline (1 to >30 mg/L)<sup>41, 42</sup>, and therefore do not inhibit  
114 bacterial growth. The samples of short-term exposure were taken after 2 h (late log-phase, T<sub>0</sub>)  
115 and 48 h (T<sub>1</sub>), respectively. To create a nutrient-depletion condition for long-term exposure,  
116 the cells were cultivated in 10-times diluted minimal medium and the culture medium was  
117 refreshed every 72 h. The samples were collected at 3 (T<sub>2</sub>), 6 (T<sub>3</sub>), 9 (T<sub>4</sub>) and 12 (T<sub>5</sub>) days.  
118 The collected cells were then harvested by centrifugation at 4000 rcf for 5 min, washed three  
119 times with sterile deionized water, and finally fixed with 70% ethanol to prevent further  
120 exposure.

## 121 2.2 Spectrochemical analysis

122 The prepared samples (minimal amount > 5  $\mu\text{L}$ ) were then applied onto Low-E slides and  
123 dried for analysis by ATR-FTIR spectroscopy. A Bruker TENSOR 27 FTIR spectrometer  
124 (Bruker Optics Ltd., UK) with a Helios ATR attachment containing a diamond internal  
125 reflection element (IRE) was applied to acquire IR spectra. The data were attained at a  
126 resolution of 3.84  $\text{cm}^{-1}$ , 2.2 kHz mirror velocity and 32 co-additions. The instrument  
127 parameters were set at 32 scans and 16  $\text{cm}^{-1}$  resolution. To collect the data, a total of 30  
128 individual spectral measurements were taken randomly from each sample using the aid of the  
129 ATR magnification-limited viewfinder camera. Prior to analysing each new specimen, the  
130 crystal was cleaned using deionized water and a background reading was taken.

## 131 2.3 Multivariate analysis and statistics

132 All the initial data generated from ATR-FTIR spectroscopy were analysed using MATLAB  
133 R2011a (*TheMathsWorks, Natick, MA, USA*) coupled with the IRootLab toolbox  
134 (<http://irootlab.googlecode.com>)<sup>43</sup>. The acquired IR spectra were merged and cut to the  
135 biochemical-cell fingerprint region (1800-900  $\text{cm}^{-1}$ ). Then a rubber-band baseline correction  
136 was applied to remove any slopes in this area. The data were then normalized to Amide I  
137 (1650  $\text{cm}^{-1}$ ) and the means were centered allowing alignment of the different spectra for  
138 comparison.

139 Principal component analysis-linear discriminant analysis (PCA-LDA) was applied  
140 after data pre-processing to reduce the number of spectra to 10 uncorrelated principal

141 components (PCs), which account for >99% of the total variance. LDA is a supervised  
142 technique coupled with PCA in order to maximize interclass and minimize intraclass  
143 variance<sup>30, 31, 44</sup>. Cross-calculation was subsequently performed to mitigate risks resulting from  
144 LDA overfitting<sup>45</sup>. The PCA-LDA loadings using ( $n-1$ ) samples ( $n$  = number of samples in  
145 dataset) was trained *via* leave-one-out cross-validation and then calculated the scores of the  
146 rest sample. This process was performed for all scores within the test.

147 PCA-LDA cluster vectors are pseudo-spectra highlighting the key biochemical  
148 alterations of each group in the dataset<sup>35</sup>, which allows one to simplify the identification of  
149 discriminating differences amongst groups. The centre of the control cluster itself is moved to  
150 the origin of the PCA-LDA factor space. The extent of peak deviation away from the origin  
151 of the factor space then occurs according to the centre of each corresponding agent-induced  
152 cluster, proportional to the discriminating extent of biochemical differences<sup>31, 45</sup>. Cluster  
153 vectors plots were also applied to indicate the most prominent six significant peaks.

154 Multivariate regression trees (MRT) were used to analyse the influence of bacterial  
155 type, exposure time and exposure category on biospectral alterations using the R package  
156 “mvpart”. Herein, Gram-positive (*M. vanbaalenii*) and Gram-negative (*P. fluorescens*) strains  
157 were assigned as 1 and 0. The exposure of AgNP, tetracycline and their mixtures were  
158 assigned as 1, 2 and 3, respectively. The samples collected at different time points (T<sub>0</sub>, T<sub>1</sub>, T<sub>2</sub>,  
159 T<sub>3</sub>, T<sub>4</sub> and T<sub>5</sub>) were assigned to 1, 2, 3, 4, 5 and 6, respectively.

160 One-way analysis of variance (ANOVA) with Tukey’s post-hoc test/or *t*-test was  
161 employed to test the differences between treatments. All statistical analyses were carried out  
162 in GraphPad Prism 6.

### 163 **3. Results and discussion**

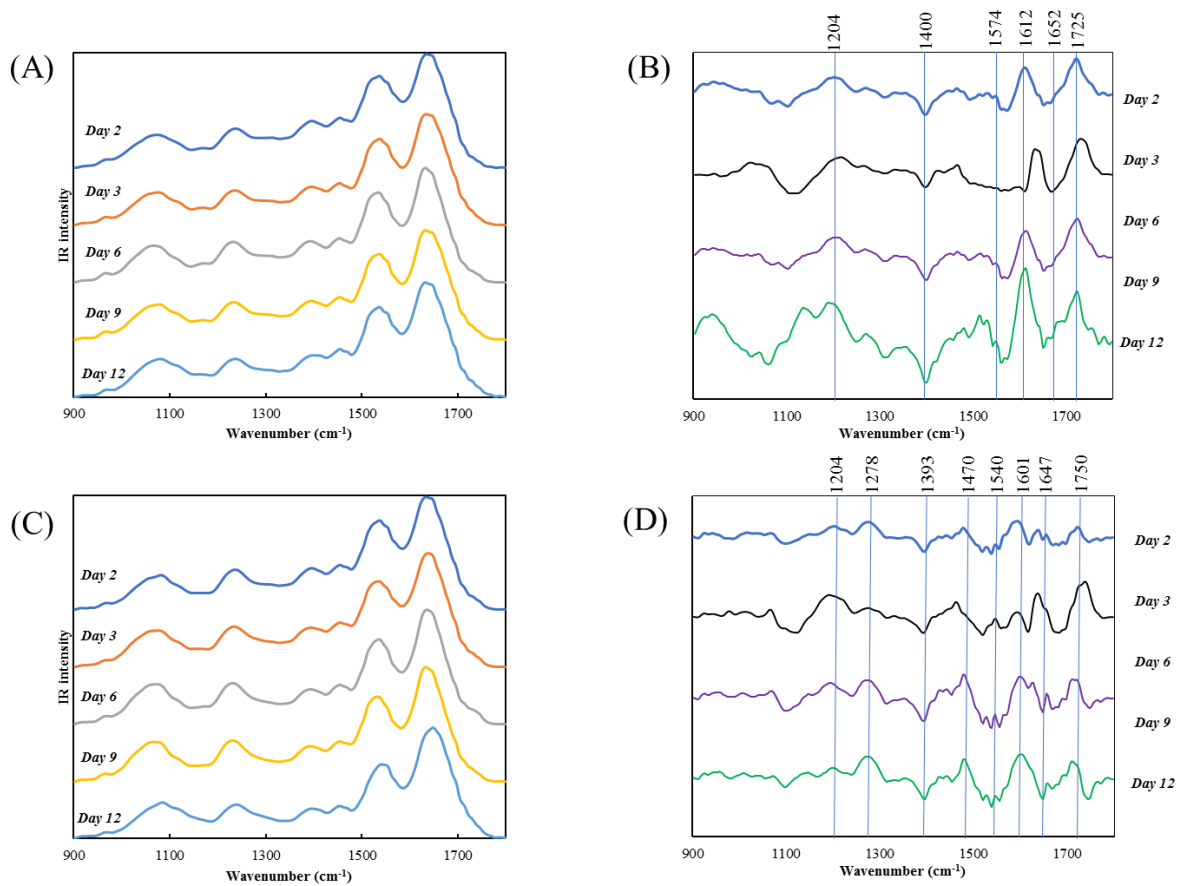
#### 164 *3.1 Growth-dependent spectrochemical alterations*

165 Throughout the study, a spectral class mean for the bacterial control group has been derived,  
166 which generates an average spectrum based on all raw data from the same group. However,  
167 minor variability is visualised from the class mean data directly between groups at different  
168 time points (Figure 1A and 1B). Although previous studies suggest that bacteria with limited  
169 nutrients are more likely to enter a dormant state waiting suitable growth conditions<sup>46, 47</sup>, the  
170 spectral alterations induced by nutrient depletion are limited. Therefore, a further cluster  
171 vectors analysis is applied to highlight the minor alterations derived from nutrient depletion



172 (Figure 1C and 1D). The identical spectral biomarkers in both Gram-positive (*M. Vanbaalenii*)  
173 and Gram-negative (*P. fluorescens*) bacteria are associated with Amide I, Amide III (~1204  
174  $\text{cm}^{-1}$ , ~1647  $\text{cm}^{-1}$ )<sup>30, 33</sup> (Table 1). The main changes appearing in *M. Vanbaalenii* are Amide  
175 III, (~1204  $\text{cm}^{-1}$ , ~1400  $\text{cm}^{-1}$ ), C=N adenine (~1574  $\text{cm}^{-1}$ ), Amide I (~1652  $\text{cm}^{-1}$ ), and C=O  
176 band (~1725  $\text{cm}^{-1}$ )<sup>33, 48</sup>. Of these, the amino acid-associated alterations possibly contributing  
177 to nucleotide metabolism, which is important for cellular catabolism are significant. Along  
178 with long-term starvation and oxygen depletion, decreasing amounts of nucleotides are  
179 associated with reduced cell activities and replication compared to log-phase. Furthermore,  
180 alterations in other cellular components (*e.g.*, proteins) might be mainly responsible for cell  
181 wall maintenance, based on previous study<sup>49</sup>.

182 The specific spectrochemical alterations of *P. fluorescens* include Amide III (~1278  
183  $\text{cm}^{-1}$ ), CH<sub>2</sub> bending of the methylene chains in lipids (~1470  $\text{cm}^{-1}$ ), protein Amide II  
184 absorption (~1540  $\text{cm}^{-1}$ ), C=N cytosine (~1601  $\text{cm}^{-1}$ ),  $\nu(\text{C}=\text{C})$  lipids, and fatty acids (~1750  
185  $\text{cm}^{-1}$ )<sup>34, 48</sup>. Accordingly, more lipid alterations under nutrient depletion conditions are found  
186 in Gram-negative *P. fluorescens* versus Gram-positive *M. vanbaalenii* owing to their  
187 differing cell wall structures. There is only a thin peptidoglycan layer (~2-3 nm) between the  
188 cytoplasmic and outer membrane in Gram-negative bacteria, whereas the outer membrane in  
189 Gram-positive bacteria is a thick peptidoglycan layer of 30 nm with no other additional  
190 structure<sup>50</sup>. The attributes of membrane structure may explain the distinct spectrochemical  
191 alterations between *P. fluorescens* and *M. vanbaalenii* under nutrient depletion, which might  
192 lead to different responses towards long-term exposure of antimicrobials.



193

194 **Figure 1.** Spectrochemical alterations with length of culture. Infrared spectra of *M.*  
 195 *vanbaalenii* (A) and *P. fluorescens* (C) from control group. Cluster vectors plots of *M.*  
 196 *vanbaalenii* (B) and *P. fluorescens* (D) from control group, indicating significant  
 197 wavenumbers contributing to segregating spectral alterations that develop with increasing  
 198 culture time.

199 **Table 1.** Spectrochemical profile regarding the significant spectral biomarkers peaks derived from cluster vectors of *M. vanbaalenii* (Gram-  
200 positive) and *P. fluorescens* (Gram-negative) post-exposure to AgNP, tetracycline and their mixtures. Red dots represent identical biomarkers for  
201 both Gram-positive and Gram-negative bacteria, and green and blue dots indicate biomarkers appear only in Gram-positive or Gram-negative  
202 bacteria, respectively.

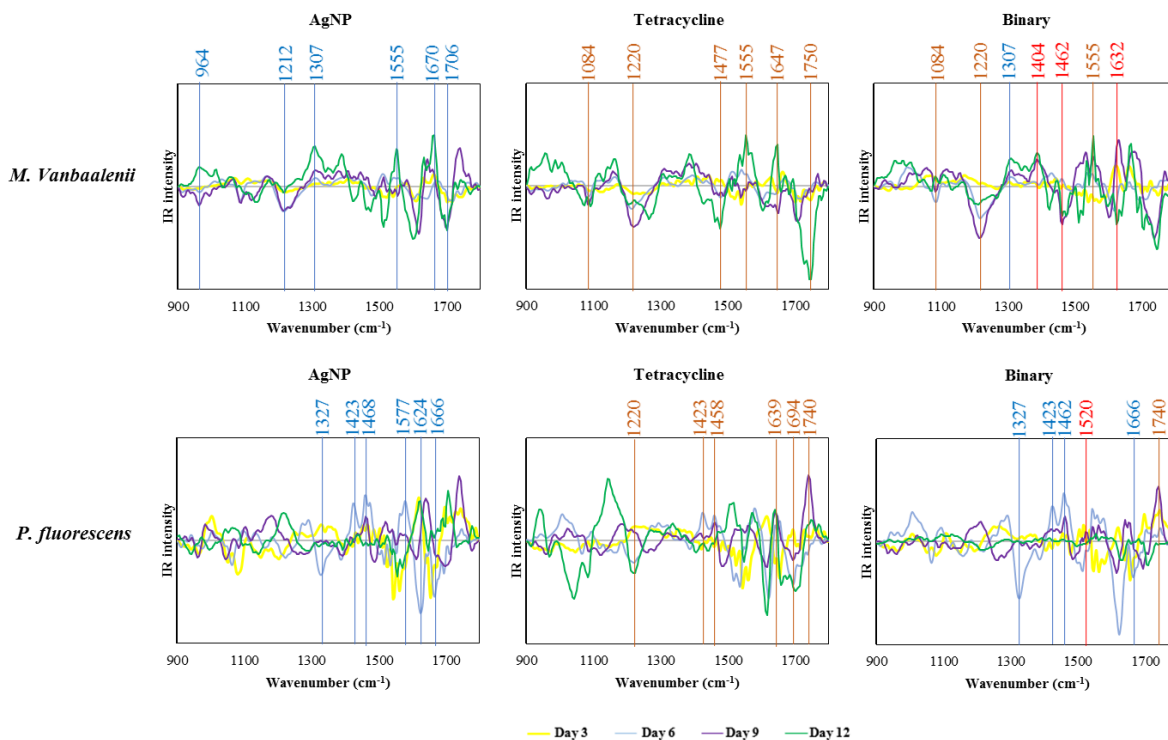
Wavenumber (cm <sup>-1</sup> )	Annotation	Gram-positive				Gram-negative			
		Growth	AgNP	Tetracycline	Binary	Growth	AgNP	Tetracycline	Binary
~ 964	C-C, C-O deoxyribose	-	●	-	-	-	-	-	-
~ 1084	DNA	-	-	●	●	-	-	-	-
~ 1204	Amide III	●	-	-	-	●	-	-	-
~ 1212	Phosphate	-	●	-	-	-	-	-	-
~ 1220	PO <sub>2</sub> <sup>-</sup> stretching in RNA and DNA	-	-	●	●	-	-	●	-
~ 1278	Amide III	-	-	-	-	●	-	-	-
~ 1307	Amide III	-	●	-	●	-	-	-	-
~ 1327	Stretching C-N thymine, adenine	-	-	-	-	-	●	-	●
~ 1393		-	-	-	-	●	-	-	-
~ 1400		●	-	-	-	-	-	-	-
~ 1404	CH <sub>3</sub> asymmetric deformation	-	-	-	●	-	-	-	-
~ 1423		-	-	-	-	-	●	●	●
~ 1458	Lipids and proteins	-	-	-	-	-	-	●	-
~ 1462		-	-	-	●	-	-	-	●
~ 1468		-	-	-	-	-	●	-	-
~ 1470	CH <sub>2</sub> bending of the methylene chains in lipids	-	-	-	-	●	-	-	-
~ 1477		-	-	●	-	-	-	-	-
~ 1520	Amide II	-	-	-	-	-	-	-	●
~ 1540	Protein amide II absorption	-	-	-	-	●	-	-	-
~ 1555	Ring base	-	●	●	●	-	-	-	-
~ 1574	C=N adenine	●	-	-	-	-	-	-	-
~ 1577	C-C stretch	-	-	-	-	-	●	-	-

~ 1601	C=N cytosine	-	-	-	-	●	-	-	-
~ 1612		●	-	-	-	-	-	-	-
~ 1624		-	-	-	-	-	●	-	-
~ 1632	C-C stretch	-	-	-	●	-	-	-	-
~ 1639	Amide	-	-	-	-	-	-	●	-
~ 1647	Amide I	-	-	●	-	●	-	-	-
~ 1652	Amide I	●	-	-	-	-	-	-	-
~ 1666	C=O stretching vibration of pyrimidine base	-	-	-	-	-	●	-	●
~ 1670	Amide I	-	●	-	-	-	-	-	-
~ 1694	Proteins	-	-	-	-	-	-	●	-
~ 1706	C=O thymine	-	●	-	-	-	-	-	-
~ 1725	C=O band	●	-	-	-	-	-	-	-
~ 1740	C=O, lipids	-	-	-	-	-	-	●	●
~ 1750	$\nu(\text{C}=\text{C})$ lipids, fatty acids	-	-	●	-	●	-	-	-

203

### 204 3.2 Spectrochemical alterations with long-term AgNP/tetracycline exposure

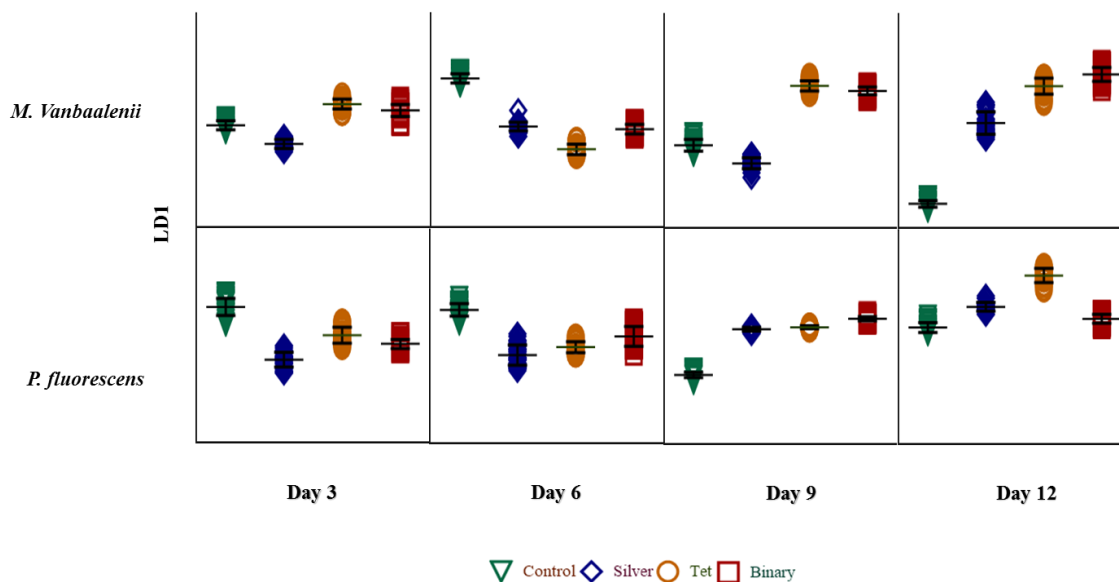
205 To identify exposure-induced alterations, the spectral data of each treatment group are  
206 compared with the control group at the same time point, eliminating the impacts of cell  
207 growth and nutrient depletion (Figure 2). In Gram-positive *M. Vanbaalenii*, the AgNP-  
208 induced alterations are C-C, C-O deoxyribose ( $\sim 964\text{ cm}^{-1}$ ), phosphate ( $\sim 1212\text{ cm}^{-1}$ ), Amide  
209 III ( $\sim 1307\text{ cm}^{-1}$ ), ring base ( $\sim 1555\text{ cm}^{-1}$ ), Amide I ( $\sim 1670\text{ cm}^{-1}$ ), and C=O thymine ( $\sim 1706$   
210  $\text{cm}^{-1}$ )<sup>30, 33, 38</sup>. Post-exposure to tetracycline, the representative peaks are DNA ( $\sim 1084\text{ cm}^{-1}$ ),  
211  $\text{PO}_2^-$  stretching in RNA and DNA ( $\sim 1220\text{ cm}^{-1}$ ), ring base ( $\sim 1555\text{ cm}^{-1}$ ), Amide I ( $\sim 1647$   
212  $\text{cm}^{-1}$ ), lipids, and fatty acids ( $\sim 1750\text{ cm}^{-1}$ )<sup>33, 38, 48</sup>. With the binary exposure, the alterations  
213 are different from individual exposures, and the specific spectral biomarkers are DNA ( $\sim 1084$   
214  $\text{cm}^{-1}$ ),  $\text{PO}_2^-$  stretching in RNA and DNA ( $\sim 1220\text{ cm}^{-1}$ ), Amide III ( $\sim 1307\text{ cm}^{-1}$ ),  $\text{CH}_3$   
215 asymmetric deformation ( $\sim 1404\text{ cm}^{-1}$ ,  $\sim 1462\text{ cm}^{-1}$ ), ring base ( $\sim 1555\text{ cm}^{-1}$ ), and C-C stretch  
216 ( $\sim 1632\text{ cm}^{-1}$ )<sup>38, 48</sup>. It is worth mentioning that the binary effects of AgNP and tetracycline on  
217 *M. vanbaalenii* spectra are mainly driven by tetracycline as more identical discriminating  
218 peaks are observed between these two groups (Table 1). To evaluate the impacts of each  
219 exposure, PCA-LDA score plots were generated and illustrate the increasing segregation  
220 between groups with increasing exposure time (from day 3 to day 12, Figure 3). Particularly,  
221 the biochemical distances of tetracycline and binary groups are co-located, apparently  
222 separated from the control group and markedly on day 12. However, the AgNP-treated  
223 groups only show slight shifting of biochemical differences compared to the control group.  
224 This result is consistent with cluster vectors analysis that the binary-exposure effects in *M.*  
225 *vanbaalenii* are closer to tetracycline alone than AgNP.



226

227 **Figure 2.** Cluster vectors plots after PCA-LDA, indicating significant wavenumbers for the  
 228 segregation of *M. vanbaalenii* and *P. fluorescens* following long-term exposure (day 3 to day  
 229 12) to AgNP, tetracycline or their mixtures.

230



231

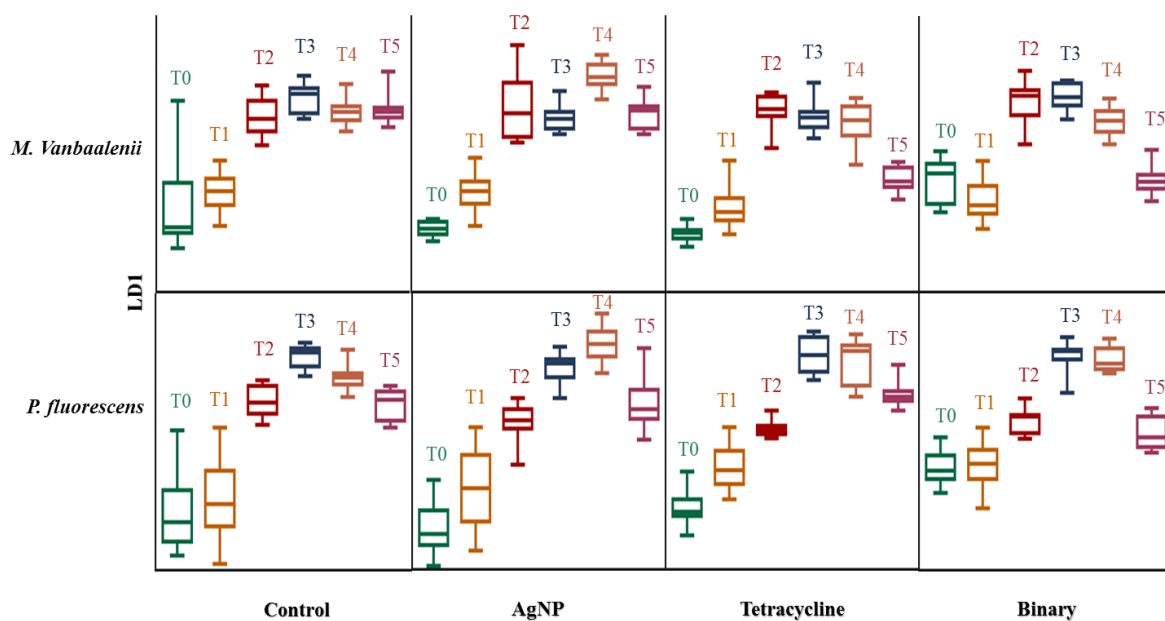
232 **Figure 3.** PCA-LDA score plots for the biospectral alteration of *M. vanbaalenii* and *P.*  
 233 *fluorescens* following long-term exposure (day 3 to day 12) to AgNP, tetracycline or their  
 234 mixtures.

235 In Gram-negative *P. fluorescens*, all the exposure groups are clearly separated from the  
236 control group in the PCA-LDA score plots (Figure 3), and there is no significant difference  
237 between each treatment. The AgNP-induced alterations include stretching C-N thymine,  
238 adenine ( $\sim 1327\text{ cm}^{-1}$ ), lipids and proteins ( $\sim 1458\text{ cm}^{-1}$ ), C-C stretch ( $\sim 1577\text{ cm}^{-1}$ ), ( $\sim 1624$   
239  $\text{cm}^{-1}$ ), and C=O stretching vibration of pyrimidine base ( $\sim 1666\text{ cm}^{-1}$ )<sup>48</sup>. The tetracycline-  
240 induced peaks are DNA ( $\sim 1220\text{ cm}^{-1}$ ); ( $\sim 1423\text{ cm}^{-1}$ ), collagen ( $\sim 1458\text{ cm}^{-1}$ ), Amide I ( $\sim 1639$   
241  $\text{cm}^{-1}$ ,  $\sim 1694\text{ cm}^{-1}$ ), and C=O lipids ( $\sim 1740\text{ cm}^{-1}$ )<sup>38, 48</sup>. Generally, outer cellular components  
242 are widely affected by both AgNP and tetracycline, including Amides I/II and proteins  
243 ( $\sim 1307\text{ cm}^{-1}$ ,  $\sim 1647\text{ cm}^{-1}$ ,  $1639\text{ -}1694\text{ cm}^{-1}$ ), and lipids and/or fatty acids ( $1750\text{ cm}^{-1}$ ,  $1458$   
244  $\text{cm}^{-1}$ ,  $1740\text{ cm}^{-1}$ )<sup>30, 33, 38, 48</sup>, indicating that the cell membrane is the primary reactive target  
245 associated with both antimicrobials which penetrate bacterial cells *via* passive diffusion and  
246 inhibit bacterial growth by perturbing protein synthesis or altering membrane structure<sup>51</sup>.  
247 Additionally, more inner cellular components are identified to be associated with tetracycline  
248 exposure than AgNP, *e.g.*, inherent DNA and RNA, possibly due to the antibiotic mechanism  
249 of tetracycline which blocks the elongation cycle by preventing incoming aminoacyl-tRNA  
250 (aa-tRNA) from binding to the ribosomal A-site and inhibiting protein synthesis<sup>52</sup>. Different  
251 from Gram-positive strains, AgNP-induced alterations contribute predominantly to the binary  
252 effects in *P. fluorescens*, *i.e.*, stretching C-N thymine, adenine ( $\sim 1327\text{ cm}^{-1}$ ,  $\sim 1423\text{ cm}^{-1}$ ,  
253  $\sim 1462\text{ cm}^{-1}$ ), Amide II ( $\sim 1520\text{ cm}^{-1}$ ), C=O stretching vibration of pyrimidine base ( $\sim 1666$   
254  $\text{cm}^{-1}$ ), and C=O lipids ( $\sim 1740\text{ cm}^{-1}$ )<sup>31, 34</sup>. These findings imply the antimicrobial synergism  
255 of AgNP and tetracycline. A previous study suggests that antibiotics' efficacy against  
256 microbes may increase in the presence of AgNP because of the bonding reaction between  
257 antibiotics and nanofillers, owing to the chelating reaction of hydroxyl and amide groups in  
258 antibiotic molecules with AgNP<sup>53</sup>.

### 259 3.3 Impacts of exposure time on spectrochemical alterations

260 Although short-term impacts by antimicrobials on bacteria is obvious and well-studied, their  
261 consequences may last for extended periods and remain unknown<sup>54</sup>. To unravel such long-  
262 term exposure effects, we measured the biospectral alterations at different time points, and  
263 found distinguishing biomarkers post-exposure to antimicrobials between short-term *versus*  
264 long-term treatments (Figure 4). Generally, in short-term exposure ( $\leq 3$  days), spectral  
265 changes are associated with components from cell membranes wherein most antimicrobial-  
266 induced alterations occur in both strains, including glycogen ( $\sim 1022\text{ cm}^{-1}$ ), symmetric  
267 phosphate stretching vibrations ( $\nu_s\text{PO}_2^-$ ;  $\sim 1088\text{ cm}^{-1}$ ,  $1092\text{ cm}^{-1}$ ), carbohydrates ( $\sim 1165$

268  $\text{cm}^{-1}$ ), protein phosphorylation ( $\sim 964 \text{ cm}^{-1}$ ), Amide I ( $\sim 1609 \text{ cm}^{-1}$ ,  $1612 \text{ cm}^{-1}$ ,  $1659 \text{ cm}^{-1}$ ,  
 269  $\sim 1670 \text{ cm}^{-1}$ ), Amide III ( $\sim 1269 \text{ cm}^{-1}$ ), COO- symmetric stretching vibrations of fatty acids  
 270 and amino acid ( $\sim 1408 \text{ cm}^{-1}$ ), proteins ( $\sim 1485 \text{ cm}^{-1}$ ,  $\sim 1550 \text{ cm}^{-1}$ ,  $\sim 1650 \text{ cm}^{-1}$ ), and lipids  
 271 ( $\sim 1701 \text{ cm}^{-1}$ ,  $1705\text{-}1750 \text{ cm}^{-1}$ )<sup>30, 32, 38, 48</sup>. Besides external cellular components, some  
 272 inherent elements are significantly influenced in long-term exposure ( $>3$  days). For instance,  
 273 long-term tetracycline-induced alterations in *P. fluorescens* include RNA and DNA (e.g.,  
 274  $\sim 1220 \text{ cm}^{-1}$ ,  $\sim 1423 \text{ cm}^{-1}$ ). Compared to prolonged exposure, short exposure induces minimal  
 275 alterations, possibly owing to bacteria undergoing pre-stage reactions against antimicrobials.  
 276 During extended exposure periods, the more obvious biospectral alterations might be  
 277 explained by increasing tetracycline accumulation *via* penetration and stronger antibiotic  
 278 effects, which prevent RNA binding to the ribosomal A-site and protein synthesis<sup>52</sup>, and  
 279 further inhibit RNA/DNA synthesis and duplication<sup>55</sup>. Another explanation is the post-  
 280 antibiotic effect (PAE) or lag of bacterial regrowth induced by long-term antimicrobial  
 281 exposure, driving bacterial entry into a growth suppression state<sup>56, 57</sup>.



282  
 283 **Figure 4.** PCA-LDA score plots of the biospectral alteration of *M. vanbaalenii* and *P.*  
 284 *fluorescens* in both short-term and long-term exposure to AgNP, tetracycline and their  
 285 mixtures. T0, T1, T2, T3, T4 and T5 represent exposure time of 2 h, 2 days, 3 days, 6 days, 9  
 286 days and 12 days, respectively.

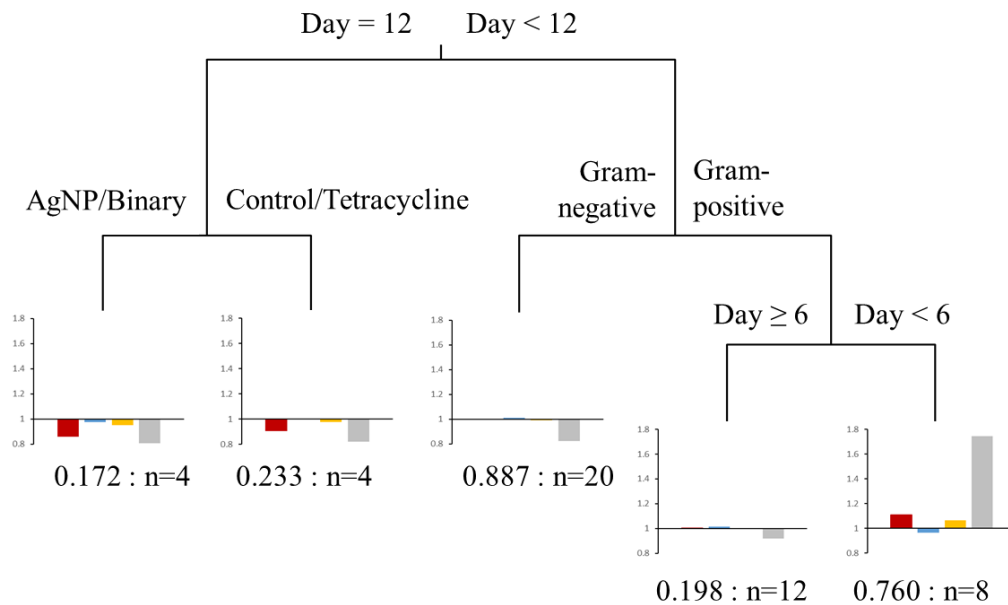
287



### 288 3.4 Influential factors determining bacterial long-term responses to antimicrobials

289 Although distinct impacts of different antimicrobials on bacteria have been well-documented,  
290 many variables including intrinsic and external factors may alter such influences in real-  
291 world scenarios. In the present study, we evaluated bacterial type, exposure category,  
292 exposure time and nutrient depletion, but which factor is the most dominating remains  
293 unclear. To answer this question, a multivariate regression trees (MRT) analysis based on  
294 isolated discriminating biomarkers is conducted to quantify the impacts of these four factors  
295 on spectral alterations. MRT visualizes these influencing factors on spectral variations in a  
296 tree with four splits based on exposure time, exposure category, bacterial type and nutrient  
297 depletion, explaining 63.7% of the total spectral variance (Figure 5). Level of influence is  
298 ranked as exposure time > exposure type > bacterial type = nutrient depletion. Exposure time  
299 accounts for 17.8% of the total variance, with the first split separating the group of 12-day  
300 exposure owing to the relatively lower intensities of DNA. In the 12-day exposure group,  
301 exposure category explains 16.1% of the variance and splits spectra into two groups of  
302 control/tetracycline and AgNP/binary, mainly based on DNA spectral biomarkers. The group  
303 of exposure <12 days is further split by bacterial type, accounting for 14.9% of the total  
304 variance and attributed to differences in DNA, phospholipid-derived fatty acids and proteins.  
305 The final split representing nutrient depletion separates the groups of 6-9 day and 0-3 day for  
306 Gram-positive bacteria (*M. vanbaalenii*, 14.9%), owing to higher cellular activities reflected  
307 by significant variations in DNA, phospholipid-derived fatty acids and proteins.

308 The MRT results are consistent with PCA-LDA score plots (Figure 4). The spectral  
309 distances of *P. fluorescens*, for instance, are similar regardless of exposure categories from  
310 day 9 due to cell regeneration against the exposure and exhibiting resistance to  
311 antimicrobials<sup>46</sup>. A prior study reported that long-term exposure (5 days) to 1 µg/L of  
312 tetracycline shows no apparent effect on cyanobacterial cells due to their natural variability in  
313 tetracycline resistance<sup>58</sup>. It might explain the closer distance between groups of control and  
314 tetracycline. Moreover, the distinct behaviours of *M. vanbaalenii* and *P. fluorescens* upon  
315 starvation can explain the fourth split in MRT, *i.e.*, *M. vanbaalenii* enters a replicative state  
316 after 6-day exposure to adapt to conditions of insufficient nutrients, whereas *P. fluorescens*  
317 appears more susceptible to nutrient depletion and starts regrowth. Evidence can be found  
318 from the additional cellular components produced in Gram-negative *P. fluorescens*, *e.g.*, fatty  
319 acids (~1750 cm<sup>-1</sup>), as their predominant energy to survive<sup>46</sup>.



Error: 0.364 CV Error: 0.572 SE: 0.119

320

321 **Figure 5.** Multivariate regression tree (MRT) analysis of environmental variables explaining  
 322 discriminating biomarkers. The scale of the sub-figures reflects the alteration degree (number  
 323 one represents the average level). Red bars represent biomarkers assigned to DNA; blue bars  
 324 represent biomarkers associated with proteins; yellow bars represent biomarkers assigned to  
 325 phospholipid-derived fatty acids; and, grey bars represent other cellular components.

326

327 Moreover, bacterial type may also have impacts on the consequences posed by antimicrobials  
 328 since bacteria differ in their cellular structures. Antimicrobials acting as both efficient  
 329 eliminators to microbes and selective agents help to propagate organisms with resistance  
 330 ability<sup>59</sup>. Herein, we found discriminating alterations between Gram-positive and Gram-  
 331 negative strains within the same exposure treatment. All the treatments exhibit distinct  
 332 alterations in Gram-positive *M. vanbaalenii* under nutrient depletion conditions (Day 3 to  
 333 Day 12), although AgNP generates very limited impact as compared to tetracycline or binary  
 334 exposure groups; these are not observed in *P. fluorescens*. The results from PCA-LDA scores  
 335 plots (Figure 3) and MRT (Figure 5) also show induced alterations in *M. vanbaalenii* are  
 336 significant compared to *P. fluorescens*. Furthermore, after long-term exposure (12 days),

337 Gram-negative *P. fluorescens* exhibit a broad range of spectral alterations assigned to lipids  
338 and/or fatty acid (*e.g.*, 1458 cm<sup>-1</sup>, 1740 cm<sup>-1</sup>), which are absent in Gram-positive *M.*  
339 *vanbaalenii*, mainly attributed to their different cell wall structures. The rigidity and extended  
340 cross-linking may reduce the target sites in cell membranes for environmental exposures and  
341 afford further protection to cells from antimicrobial penetration<sup>12, 53</sup>. It implies that cell  
342 membranes of Gram-negative bacteria are more likely to be influenced compared to Gram-  
343 positive bacteria under certain antibacterial treatments (*e.g.*, AgNP)<sup>12, 50, 60</sup>. Past studies report  
344 the oxidation of smaller AgNPs (1-10 nm) by intercellular reactive oxygen species (ROS) in  
345 Gram-negative bacteria, resulting in the release of silver ions during AgNP penetration  
346 through the cell membrane and entrance into the cytoplasm<sup>60</sup>. These silver ions could be  
347 further transferred to other Gram-negative bacterial cells, the membrane and cytoplasm which  
348 contain many sulfur-containing proteins for the released Ag<sup>+</sup> to bind to and inactivate<sup>50, 60</sup>.  
349 Furthermore, it has been recognised that heavy metal treatment can induce global  
350 biomolecular changes in lipids and proteins, implying exotic exposure may lead to the  
351 development of relevant metabolic changes in cellular components, particularly the  
352 membrane<sup>61-63</sup>. A recent study, for instance, reported that Ag exposure could increase cellular  
353 lipid contents while decrease membrane fluidity<sup>61</sup>, and the possible mechanism is upregulated  
354 lipid biosynthesis, which is known to be associated with the reduced membrane permeability.

355 Besides bacterial type, exposure time and exposure category, nutrient depletion is also  
356 found to be an influential factor in the bacterial antimicrobial response. Here, bacterial cells  
357 tend to adapt to new environmental stimuli after entering into a long-term nutrient-deprived  
358 situation. From the cluster vectors analysis (Figure 1), spectral alterations in both strains from  
359 Day 6 show slight peak shifts, which can be regarded as a potential signal showing that  
360 bacterial cells are undergoing adaption. Additionally, *M. vanbaalenii* becomes a persistent  
361 suspension in the media on entering a dormant state from Day 6. This is because bacteria in a  
362 non-growing state can survive for much longer time under conditions of reduced oxygen or  
363 nutrient deprivation<sup>46, 47</sup>. Upon starvation, bacterial cells fragment into small spheroids  
364 exhibiting rapid and drastic decreases in endogenous metabolism. This reorganization gives  
365 bacteria maximum survival during long-term starvation. Specifically, bacteria on starvation  
366 initially induce dwarfing generating cell number increases *via* fragmentation over the first 1  
367 to 2 h and continuous size reductions in the fragmented cells, but no further increase in  
368 numbers. After dwarfing phases, cell size continues to get smaller, with little or no metabolic  
369 activity, and slow loss of viability<sup>64</sup>. It has been reported that non-growing phase bacteria

370 adapt to and increase their tolerance to environmental stresses and such developed persistent  
371 bacilli are capable of surviving several months of combinatorial antibiotic treatment<sup>47</sup>, which  
372 implies that stressed living conditions, to some extent and paradoxically, could help microbial  
373 resistance to antimicrobial effects.

#### 374 **4. Conclusions**

375 In the present study, we employed spectrochemical analysis coupled with multivariate  
376 analysis as a robust tool towards investigating bacterial responses<sup>65</sup> to long-term and low-  
377 level exposure of antimicrobials under nutrient depletion conditions. ATR-FTIR spectroscopy  
378 shows feasibility in revealing sufficient biochemical information continuously even at  
379 extremely low-level exposures in a starvation situation, which fits better with real-world  
380 circumstances and the natural state of microcosms. From the multivariate analysis of spectra  
381 coupled with MRT, we evaluate the significance of different factors on long-term bacterial  
382 responses to antimicrobials and find pivotal roles for exposure time and nutrient depletion.  
383 Nutrient depletion can drive bacterial cells to either enter into a dormant state or exhibit  
384 extra-cellular components against environmental antimicrobials, consequently causing a  
385 broader range of spectral alteration compared to short-term exposures. Differences in  
386 bacterial behaviours towards antimicrobials are also found between bacterial types (Gram-  
387 positive *versus* Gram-negative) attributed to variations in cell wall structure. Our work is the  
388 first revealing of the more important roles of exposure duration and nutrient depletion, rather  
389 than of antimicrobial reagents, on microbial responses to low-level and prolonged  
390 environmental exposures. We believe this approach has an important future with potential  
391 feasibility in *in situ* screening of environmental exposures in real-time.

#### 392 **Conflicts of interest**

393 There are no conflicts of interest to declare.

#### 394 **Acknowledgement**

395 N.J. was funded by Chinese Academy of Sciences and China Scholarship Council.

396

397

398

399 **References**

- 400 1. J. Conly, *Can. Med. Assoc. J.*, 2002, **167**, 885-891.
- 401 2. J. W. Harrison and T. A. Svec, *Quintessence Int.*, 1998, **29**, 223-229.
- 402 3. J. C. Chee-Sanford, R. I. Aminov, I. J. Krapac, N. Garrigues-Jeanjean and R. I.  
403 Mackie, *Appl. Environ. Microbiol.*, 2001, **67**, 1494-1502.
- 404 4. G. Hamscher, S. Sczesny, H. Hoper and H. Nau, *Anal Chem*, 2002, **74**, 1509-1518.
- 405 5. X. L. Ji, Q. H. Shen, F. Liu, J. Ma, G. Xu, Y. L. Wang and M. H. Wu, *J. Hazard*  
406 *Mater.*, 2012, **235**, 178-185.
- 407 6. L. Cantas, S. Q. A. Shah, L. M. Cavaco, C. M. Manaia, F. Walsh, M. Popowska, H.  
408 Garelick, H. Burgmann and H. Sorum, *Front. Microbiol.*, 2013, **4**, 14.
- 409 7. A. Koluman and A. Dikici, *Crit. Rev. Microbiol.*, 2013, **39**, 57-69.
- 410 8. M. Tandukar, S. Oh, U. Tezel, K. T. Konstantinidis and S. G. Pavlostathis, *Environ.*  
411 *Sci. Technol.*, 2013, **47**, 9730-9738.
- 412 9. J. L. Martinez and F. Baquero, *Ups. J. Med. Sci.*, 2014, **119**, 68-77.
- 413 10. J. S. Kim, E. Kuk, K. N. Yu, J. H. Kim, S. J. Park, H. J. Lee, S. H. Kim, Y. K. Park, Y.  
414 H. Park, C. Y. Hwang, Y. K. Kim, Y. S. Lee, D. H. Jeong and M. H. Cho, *Nanomed.-*  
415 *Nanotechnol. Biol. Med.*, 2014, **10**, 1119-1119.
- 416 11. C. N. Lok, C. M. Ho, R. Chen, Q. Y. He, W. Y. Yu, H. Sun, P. K. H. Tam, J. F. Chiu  
417 and C. M. Che, *J. Biol. Inorg. Chem.*, 2007, **12**, 527-534.
- 418 12. H. H. Lara, N. V. Ayala-Nunez, L. D. I. Turrent and C. R. Padilla, *World J. Microbiol.*  
419 *Biotechnol.*, 2010, **26**, 615-621.
- 420 13. C. Marambio-Jones and E. M. V. Hoek, *J. Nanopart. Res.*, 2010, **12**, 1531-1551.
- 421 14. R. J. Griffitt, N. J. Brown-Peterson, D. A. Savin, C. S. Manning, I. Boube, R. A. Ryan  
422 and M. Brouwer, *Environ. Toxicol. Chem.*, 2012, **31**, 160-167.
- 423 15. A. Gupta and S. Silver, *Nat. Biotechnol.*, 1998, **16**, 888-888.
- 424 16. N. F. Jin, D. Y. Zhang and F. L. Martin, *Integr. Biol.*, 2017, **9**, 406-417.
- 425 17. P. Marschner, C. H. Yang, R. Lieberei and D. E. Crowley, *Soil Biol Biochem*, 2001,  
426 **33**, 1437-1445.
- 427 18. E. K. Costello, C. L. Lauber, M. Hamady, N. Fierer, J. I. Gordon and R. Knight,  
428 *Science*, 2009, **326**, 1694-1697.
- 429 19. C. L. Lauber, M. Hamady, R. Knight and N. Fierer, *Appl. Environ. Microbiol.*, 2009,  
430 **75**, 5111-5120.
- 431 20. M. Wietz, B. Wemheuer, H. Simon, H. A. Giebel, M. A. Seibt, R. Daniel, T.  
432 Brinkhoff and M. Simon, *Environ. Microbiol.*, 2015, **17**, 3822-3831.
- 433 21. H. Li, F. L. Martin and D. Y. Zhang, *Anal. Chem.*, 2017, **89**, 3909-3918.
- 434 22. P. S. Stewart and J. W. Costerton, *Lancet*, 2001, **358**, 135-138.
- 435 23. N. Hoiby, T. Bjarnsholt, M. Givskov, S. Molin and O. Ciofu, *Int. J. Antimicrob.*  
436 *Agents*, 2010, **35**, 322-332.
- 437 24. C. G. Mayhall and E. Apollo, *Antimicrob. Agents Chemother.*, 1980, **18**, 784-788.
- 438 25. M. R. W. Brown, D. G. Allison and P. Gilbert, *J. Antimicrob. Chemother.*, 1988, **22**,  
439 777-780.
- 440 26. S. M. Ede, L. M. Hafner and P. M. Fredericks, *Appl. Spectrosc.*, 2004, **58**, 317-322.
- 441 27. O. I. Kalantzi, R. Hewitt, K. J. Ford, L. Cooper, R. E. Alcock, G. O. Thomas, J. A.  
442 Morris, T. J. McMillan, K. C. Jones and F. L. Martin, *Carcinogenesis*, 2004, **25**, 613-  
443 622.
- 444 28. J. L. Barber, M. J. Walsh, R. Hewitt, K. C. Jones and F. L. Martin, *Mutagenesis*, 2006,  
445 **21**, 351-360.
- 446 29. O. Fridman, A. Goldberg, I. Ronin, N. Shores and N. Q. Balaban, *Nature*, 2014, **513**,  
447 418-421.

- 448 30. F. L. Martin, J. G. Kelly, V. Llabjani, P. L. Martin-Hirsch, Patel, II, J. Trevisan, N. J.  
449 Fullwood and M. J. Walsh, *Nat. Protoc.*, 2010, **5**, 1748-1760.
- 450 31. M. J. Riding, F. L. Martin, J. Trevisan, V. Llabjani, Patel, II, K. C. Jones and K. T.  
451 Semple, *Environ. Pollut.*, 2012, **163**, 226-234.
- 452 32. J. Li, R. Strong, J. Trevisan, S. W. Fogarty, N. J. Fullwood, K. C. Jones and F. L.  
453 Martin, *Environ. Sci. Technol.*, 2013, **47**, 10005-10011.
- 454 33. M. J. Baker, J. Trevisan, P. Bassan, R. Bhargava, H. J. Butler, K. M. Dorling, P. R.  
455 Fielden, S. W. Fogarty, N. J. Fullwood, K. A. Heys, C. Hughes, P. Lasch, P. L.  
456 Martin-Hirsch, B. Obinaju, G. D. Sockalingum, J. Sule-Suso, R. J. Strong, M. J.  
457 Walsh, B. R. Wood, P. Gardner and F. L. Martin, *Nat. Protoc.*, 2014, **9**, 1771-1791.
- 458 34. K. A. Heys, M. J. Riding, R. J. Strong, R. F. Shore, M. G. Pereira, K. C. Jones, K. T.  
459 Semple and F. L. Martin, *Analyt.*, 2014, **139**, 896-905.
- 460 35. J. G. Kelly, J. Trevisan, A. D. Scott, P. L. Carmichael, H. M. Pollock, P. L. Martin-  
461 Hirsch and F. L. Martin, *J. Proteome Res.*, 2011, **10**, 1437-1448.
- 462 36. J. Trevisan, P. P. Angelov, P. L. Carmichael, A. D. Scott and F. L. Martin, *Analyt.*,  
463 2012, **137**, 3202-3215.
- 464 37. N. Jin, M. Paraskevaïdi, K. T. Semple, F. L. Martin and D. Y. Zhang, *Anal Chem*,  
465 2017, **89**, 9814-9821.
- 466 38. N. Jin, K. T. Semple, L. Jiang, C. Luo, D. Zhang and F. L. Martin, *Analyt.*, 2018, **143**,  
467 768-776.
- 468 39. S. N. El Din, T. A. El-Tayeb, K. Abou-Aïsha and M. El-Azizi, *Int. J. Nanomed.*, 2016,  
469 **11**, 1749-1758.
- 470 40. A. J. Kora and J. Arunachalam, *World J. Microbiol. Biotechnol.*, 2011, **27**, 1209-1216.
- 471 41. J. T. H. Jo, F. S. L. Brinkman and R. E. W. Hancock, *Antimicrob. Agents Chemother.*,  
472 2003, **47**, 1101-1111.
- 473 42. H. Wu, X. Shi, H. Wang and J. Liu, *J. Antimicrob. Chemother.*, 2000, **46**, 121-123.
- 474 43. J. Trevisan, P. P. Angelov, A. D. Scott, P. L. Carmichael and F. L. Martin,  
475 *Bioinformatics*, 2013, **29**, 1095-1097.
- 476 44. F. L. Martin, M. J. German, E. Wit, T. Fearn, N. Ragavan and H. M. Pollock, *J.*  
477 *Comput. Biol.*, 2007, **14**, 1176-1184.
- 478 45. J. Li, G. G. Ying, K. C. Jones and F. L. Martin, *Analyt.*, 2015, **140**, 2687-2695.
- 479 46. J. C. Betts, P. T. Lukey, L. C. Robb, R. A. McAdam and K. Duncan, *Mol. Microbiol.*,  
480 2002, **43**, 717-731.
- 481 47. T. Hampshire, S. Soneji, J. Bacon, B. W. James, J. Hinds, K. Laing, R. A. Stabler, P.  
482 D. Marsh and P. D. Butcher, *Tuberculosis*, 2004, **84**, 228-238.
- 483 48. Z. Movasaghi, S. Rehman and I. U. Rehman, *Appl. Spectrosc. Rev.*, 2008, **43**, 134-  
484 179.
- 485 49. M. Drapal, P. R. Wheeler and P. D. Fraser, *Microbiology-(UK)*, 2016, **162**, 1456-1467.
- 486 50. J. R. Morones, J. L. Elechiguerra, A. Camacho, K. Holt, J. B. Kouri, J. T. Ramirez  
487 and M. J. Yacaman, *Nanotechnology*, 2005, **16**, 2346-2353.
- 488 51. D. Schnappinger and W. Hillen, *Arch. Microbiol.*, 1996, **165**, 359-369.
- 489 52. S. R. Connell, C. A. Trieber, G. P. Dinos, E. Einfeldt, D. E. Taylor and K. H.  
490 Nierhaus, *Embo J.*, 2003, **22**, 945-953.
- 491 53. A. M. Fayaz, K. Balaji, M. Girilal, R. Yadav, P. T. Kalaichelvan and R. Venketesan,  
492 *Nanomed.-Nanotechnol. Biol. Med.*, 2010, **6**, 103-109.
- 493 54. C. Jernberg, S. Lofmark, C. Edlund and J. K. Jansson, *Microbiology-(UK)*, 2010, **156**,  
494 3216-3223.
- 495 55. M. Argast and C. F. Beck, *Antimicrob. Agents Chemother.*, 1984, **26**, 263-265.
- 496 56. R. W. Bundtzen, A. U. Gerber, D. L. Cohn and W. A. Craig, *Rev. Infect. Dis.*, 1981, **3**,  
497 28-37.

- 498 57. K. Fursted, A. Hjort and L. Knudsen, *J. Antimicrob. Chemother.*, 1997, **40**, 221-226.  
499 58. F. Pomati, A. G. Netting, D. Calamari and B. A. Neilan, *Aquat. Toxicol.*, 2004, **67**,  
500 387-396.  
501 59. S. B. Levy, *J. Antimicrob. Chemother.*, 2002, **49**, 25-30.  
502 60. Z. M. Xiu, J. Ma and P. J. J. Alvarez, *Environ Sci Technol*, 2011, **45**, 9003-9008.  
503 61. R. Gurbanov, S. N. Ozek, S. Tunçer, F. Severcan and A. G. Gozen, *J. Biophotonics*,  
504 2017, Doi: 10.1002/jbio.201700252.  
505 62. R. Gurbanov, N. Simsek Ozek, A. G. Gozen and F. Severcan, *Anal Chem*, 2015, **87**,  
506 9653-9661.  
507 63. M. Kardas, A. G. Gozen and F. Severcan, *Aquat Toxicol*, 2014, **155**, 15-23.  
508 64. S. Kjelleberg, B. A. Humphrey and K. C. Marshall, *Appl. Environ. Microbiol.*, 1983,  
509 **46**, 978-984.  
510 65. M. J. Riding, J. Trevisan, C. J. Hirschmugl, K. C. Jones, K. T. Semple and F. L.  
511 Martin, *Environ. Int.*, 2012, **50**, 56-65.  
512  
513